JURNAL REKAYASA MESIN
Universitas Brawijaya

About the Journal

Rekayasa Mesin is published by the Mechanical Engineering Department, Faculty of Engineering, Brawijaya, Malang, East Java, Indonesia. **Rekayasa Mesin** is an open-access, peer-reviewed journal that mediates the dissemination of academicians, researchers, and practitioners in mechanical engineering. **Rekayasa Mesin** accepts submission from all over the world, especially from Indonesia.

Rekayasa Mesin aims to provide a forum for national and international academicians, researchers, and practitioners on mechanical engineering to publish original articles. All accepted articles will be published and will be freely available to all readers with worldwide visibility and coverage.

The scope of **Rekayasa Mesin** is **specific topics and issues** in mechanical engineering such as design, energy conversion, manufacture, and metallurgy.

In terms of plagiarism and self-plagiarism, the similarity index from multiple sources **should not exceed 20%** and from a single source **should not exceed 5%**. **Rekayasa Mesin** uses a plagiarism detector to screen articles for detecting plagiarism. Detection of overlapping and similar text is used there, and so quotations and appropriate citations have to be used whenever required.

All articles submitted to this journal can be written in **English**.

Rekayasa Mesin has been indexed in the **Directory of Open Access Journals (DOAJ)**, **SINTA**, **Google Scholar**, and **Garba Rujukan Digital (GARUDA).**

Rekayasa Mesin has been nationally **re-accredited** by the Ministry of Research and Technology/ National Research and Innovation Agency of the Republic of Indonesia (Volume 16 No. 1 2025 - Volume 20 No. 2 2029) and indexed in **SINTA 2.**

Decree No. **0110/C3/DT.05.00/2026 on February 3rd, 2026**

P-ISSN 2338-1663 | **E-ISSN** 2477-6041 | **DOI prefix** 10.21776/ub.jrm

---

Full English Publication Policy Starting Volume 17 No. 1 (2026)

2026-02-25

Dear Authors,

To enhance the international visibility and academic quality of *Rekayasa Mesin Journal*, starting from Volume 17 No. 1 (2026), all articles published in the journal will be written entirely in English.

This policy is implemented as part of our preparation for SCOPUS indexation in 2026 and to strengthen the journal's global reach, readership, and citation impact. Publishing in English will allow wider dissemination of research findings and improve international collaboration opportunities.

For manuscripts that have already been submitted or accepted in Bahasa Indonesia, authors are kindly requested to translate and revise their articles into English before proceeding to the final submission and publication stage. The editorial team will coordinate directly with authors to ensure a smooth transition.

We sincerely thank you for your continued trust in publishing your research in *Rekayasa Mesin*. We look forward to receiving your high-quality contributions in English.

Read More >

Reaccredited of Rekayasa Mesin 2025 - 2029
2026-02-25

New Template for Rekayasa Mesin Publication
2023-06-02

Email Address of Author
2022-02-17

Reaccredited of Rekayasa Mesin 2020 - 2025
2021-02-21

Journal Subscription
2016-08-26

Current Issue

Vol. 17 No. 1 (2026)

DOI: https://doi.org/10.21776/jrm.v17i1

Published: 2026-05-26

Articles

The Effect of Friction Spot Stir Welding in Installing Double Cover Rivet Lap Joints on Aluminum 2024 – T3 and 7075 – T6 with Mechanical Strength

Sehono Sehono, Febrian Adi Wibisono, Ikbal Rizki Putra

1-12

PDF

Effect of Air Flow on Drying Stevia Rebaudiana using Solar Dryer Greenhouse

Vivi Nurhadianty, Luthfi Kurnia Dewi, Aji Hendra Sarosa, Moch Fitron Muttaqim, Fahrul Huzain Hidayat

13-21

PDF

Influence of Anodizing Parameters on Surface Hardness of Recast Al6061 for Hexapod Fixator Ring Development

Iffa Azzahra Firdaus, Ilham Priadythama , R Hari Setyanto

23-32

PDF

Validation of Experimental Study and SimulationOTEC Power Plant using Shell-Tube Heat Exchanger Materials with Copper, Tin, and Working Fluid Ammonia

Mawardi Mawardi, Zufri Hasrudy Siregar, Yoga Tri Nugraha, Rizkha Rida, Tengku Muhammad Fahri , Muhammad Irwanto

33-44

PDF

Comparative Analysis of Creep Deformation in Ferritic Martensitic Steel Across BM, WJ, and HAZ Regions at 570°C

I Made Wicaksana Ekaputra

45-54

PDF

Analysis of Surface Roughness Parameters of Copper Alloy Ring Synchronizer Outer Components Fabricated by CNC Turning on the Okuma 2SP-150H Lathe

Aries Abbas, Alfian Ady Saputra

55-63

PDF

The Effect of Minimum Quantity Lubrication (MQL) and Depth of Cut on Surface Roughness in Turning of AISI 1020 Steel

Rahul Rahul, Muhammad Rismanto, Muhammad Iqbal, Awal Syahrani Sirajuddin, Anjar Asmara, Jumadil Hair
65-73

PDF

Biosurfactant-Assisted Hydrogen Evolution: Effects of Sapindus Rarak Extract on Alkaline Electrolysis Performance

Mardi Santoso, David Fernando Sinurat, Anton Royanto Ahmad, Nurkholis Hamidi, Purnami Purnami
75-87

PDF

Optimization of Solar Panel Tilt for Enhanced Electrical Power Output based on Solar Radiation Variations in Cilacap

Christian Soolany, Nur Aji Bangkit Barkah Pangestu , Didi Zinedine Waluyo , Setya Permana Sutisna
89-98

PDF

Effect of Pyrolysis Temperature Variation on Optimization of Tobacco Stalk Biochar Characteristics

Kosjoko Kosjoko, Asroful Abidin, Danang Kumara Hadi, Fitriana Dina Rizkina
99-112

PDF

Effect of High Concentration Alkali Treatment on the Mechanical and Structural Properties of Doyo Fibers (Curculigo Latifolia)

Ferry Bayu Setiawan, Putu Hadi Setyarini, Yudy Surya Irawan
113-123

PDF

Design of a Portable Quick-Release Drive System for Conventional Manual Wheelchairs to Enhance Comfort and Accessibility

Rolan Siregar, Michael Owen , Samuel Parsadaanta Purba
125-132

PDF

Process–Composition–Property Relationships of Blended Coconut Shell–Teak Leaf (Tectona Grandis) Powder Biochar Briquettes for Solid Renewable Fuel Applications

Kukuh Andreng Pangestu, Harwin Saptoadi
133-148

PDF

Design and Structural Performance Evaluation of a Motorcycle Disc Brake Testing Device using Finite Element Method

I Nyoman Bramastra Yana, Ery Muthoriq , Gunawan Gunawan, Dwi Wahyu Hidayat

149-160

PDF

Comparative Analysis of Structure and Material of Absorption Box on Rear Underrun Protection Device using Simple Additive Weighting

Rizki Nabil Reyhan, Ethys Pranoto, Frans Tohom, Ery Muthoriq, Dwi Wahyu Hidayat

161-178

PDF

View All Issues

Open Journal Systems

Language

English

Make a Submission

About Rekayasa Mesin

Focus and Scope

Editorial Team

Reviewer Acknowledgement

Publication Ethics

Abstracting and Indexing

Visitor Statistics

Author Fees

Tools

MENDELEY

Mendeley User Guide

Insert Citation using Mendeley

grammarly

THOMSON REUTERS
ENDNOTE

Index

DOAJ DIRECTORY OF OPEN ACCESS JOURNALS

sinta Science and Technology Index S2

In Collaboration With

PERKINDO

Profesional dalam Berkarya

Information for Author

Author Guidelines

Template

Article Example for New Template

Online Submissions (pdf)

Video Guidelines:

* Register

* Login and Submission

* Editor Respon 1

* Author merevisi

* Finishing Editorial

* Assign Reviewer

* Reviewer External

* Meneruskan Review

* Revisi dari Reviewer

* Editor Respon 2

Information

For Readers

For Authors

For Librarians

JURNAL REKAYASA MESIN
Universitas Brawijaya

Home / Editorial Team

Editorial Team

Vol. 17. No.1

ISSN 2477-6041 articles 5, pp. 45 – 54, 2026

COMPARATIVE ANALYSIS OF CREEP DEFORMATION IN FERRITIC MARTENSITIC STEEL ACROSS BM, WJ, AND HAZ REGIONS AT 570°C

I.M.W. Ekaputra [1)]

[1)]**Jurusan Teknik Mesin**
Universitas Sanata Dharma
Paingan, Krodan, Maguwoharjo, Kec. Depok, Kabupaten Sleman, Daerah Istimewa Yogyakarta 55281, INDONESIA
made@usd.ac.id

Abstract

Creep is a time-dependent deformation in which failure can occur in years. The probabilistic assessment was a typical method for predicting creep deformation. The prediction was conducted by extrapolating the short-time creep laboratory test to the long-time data. A small deviation of extrapolation data was expected. Hence, a large number of creep tests were needed, since deviations in material properties cannot be avoided, especially in welded materials. In this study, the creep strain rate of Gr-91 steel was compared among the base metal (BM), weld joint (WJ), and heat-affected zone (HAZ). Welded steel was manufactured by the tungsten inert gas welding method. The creep test was conducted for each of the BM, WJ, and HAZ specimens using a lever-arm-type creep machine, following ASTM E139. The homologous creep temperature was set at 570 °C for a series of constant load ranges from 250 to 160 MPa. The strain-time curves of BM, WJ, and HAZ were generated after the specimens were fractured. The trend line of the creep strain rate is then determined using Norton's equation. The creep mechanism of BM, WJ, and HAZ was investigated based on the creep exponent and strain hardening coefficient obtained from Norton's equation.

Keywords: *Creep Deformation, Gr-91, HAZ, Norton's Equation.*

1. INTRODUCTION

Fossil fuels remain the primary energy source currently used in many countries. Nearly 80% of the energy produced comes from fossil fuels, such as coal and petroleum [1], [2]. The availability of fossil fuels and the environmental impacts (carbon footprints and greenhouse gas emissions) have become global issues [3]. New and renewable energy sources are essential as replacements for fossil-fuel-based energy. Fourth-Generation Nuclear Power Plants (NPPs) have been developed as an advanced new energy technology solution. Generation IV NPPs are capable of meeting future energy needs efficiently, safely, and in an environmentally friendly manner [1], [3], [4]. This generation offers significant advantages over previous-generation NPPs through innovative reactor designs, higher thermal efficiency, and more reliable passive safety systems. Generation IV NPPs are designed to minimize nuclear waste and support more efficient use of nuclear fuel, in line with sustainable development.

One of the main challenges in the development of Generation IV NPPs is selecting structural materials. The material must withstand operating at high temperatures and in extreme radiation environments. These materials must be resistant to long-term

Corresponding Author:
✉ **I Made Wicaksana Ekaputra**
Received on: 2025-03-05
Revised on: 2026-03-14
Accepted on: 2026-03-17

DOI: 10.21776/jrm.v17i1.2071

deformation (creep), corrosion, and oxidation, and must maintain microstructural stability under intensive operating conditions. Generation IV reactors were developed to extend the operational lifespan of previous-generation nuclear power plants, which was around 30 years, to as long as 70 years [5], [6]. Safety concerns have become a primary consideration, particularly following the 2011 accident at one of the reactors at the Fukushima Daiichi plant [7]. The evaluation methods used to estimate deformation rates and creep mechanisms are a key topic requiring re-examination [8]. Long-term creep deformation can cause significant microstructural changes, leading to material degradation. Accurate prediction methods are essential for assessing the extent of degradation [9]. Predicting long-term deformation mechanisms can be based on the results of short-term laboratory tests. Short-term laboratory testing is a stage used to investigate the mechanisms of creep deformation [10]. Deformation mechanisms can be linked to several creep test results, such as strain rate, fracture life, ductility, and fracture type.

Ferritic-martensitic steel is one of the leading candidates for key components in Generation IV nuclear power plants of the very high-temperature reactor (VHTR) type [11], [12]. This type of steel is used in several components of the VHTR, such as the pressure vessel and the boiler. Ferritic-martensitic steel consists of several main components, namely iron (Fe), carbon (C), chromium (Cr), and molybdenum (Mo) [11]. The chromium component in the alloy gives ferritic-martensitic steel good resistance to high-temperature environments. The pressure vessel components in the VHTR operate at temperatures up to 600 °C. The formation of ferritic-martensitic steel alloys occurs via an interstitial solid-solution mechanism with low levels of carbon and nitrogen. With the addition of these components, ferritic-martensitic steel alloys also exhibit resistance to stress-corrosion cracking (SCC). One of the ferritic-martensitic steel grades under consideration for use in VHTR components is Grade 91 (Gr-91).

In addition to selecting the appropriate material, the manufacturing process, such as joining, is another challenge that requires further investigation. Fusion welding is a viable method for ferritic-martensitic steel. However, one challenge with this welding process is the formation of non-uniform phases, particularly in the heat-affected zone (HAZ), which can degrade mechanical properties [13]. The non-uniformity of the phases formed in the HAZ can result in a higher creep deformation rate than in unwelded material. It has been reported that the phase inhomogeneity formed in the HAZ causes Type-IV cracks, as shown in Figure 1(a) [14], [15]. Meanwhile, Figure 1(b) shows Type-I cracks occurring in the base metal (BM) or weld joint (WJ). A comprehensive investigation into creep deformation in ferritic-martensitic steel, particularly in welded components for VHTRs operating at 500-600 °C, is needed. Specific testing must be performed to ensure that predictions of creep failure exhibit minimal deviation.

In this study, creep testing of Gr-91 welded ferritic-martensitic steel was investigated. The creep testing followed the ASTM E139 standard. A constant load was applied within a range of 250 to 160 MPa. During each load application, the furnace temperature was maintained at 570°C. The creep test data, in the form of stress-strain curves, were obtained after each specimen failed. Based on these curves, the creep deformation characteristics of the BM, WJ, and HAZ specimens could be determined and compared.

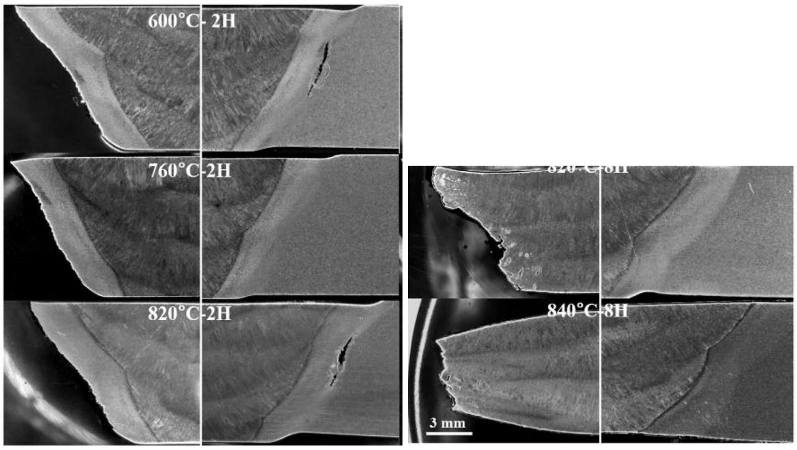

(a) (b)

Figure 1. Fracture type of creep failure: (a) type-IV, (b) type I.

The creep deformation characteristics of each specimen were evaluated based on the creep exponent and strain hardening coefficient derived from the stress-strain curves. The Norton equation was applied to generate a trendline on the stress-strain curves.

2. METHOD

The raw material used in this study was in the form of plates obtained from a rolling process. The rolled plates had a final thickness of 30 mm. Before being processed into cylindrical specimens, the plates were normalized at 1000 °C for 45 minutes. The composition of Gr-91 refers to the composition specified in the ASME T9 standard [16]. The composition of Gr-91 is shown in Table 1. The plate was welded using the tungsten inert gas (TIG) process. Figure 2 shows a cross-section of the welded Gr-91 plate. There are three areas in the weld: BM, WJ, and HAZ. Cylindrical creep specimens were prepared based on each of these areas. Figure 3 shows the dimensions of the creep specimens used in this study.

The standard used for the creep test is ASTM E139 [17]. The cylindrical specimens used had a diameter of 6 mm and a gauge length of 30 mm. The creep test was conducted using a lever-arm machine with a load ratio of 1:20. Each specimen was placed in a heating furnace and loaded from 250 to 160 MPa at 570°C. In accordance with the creep testing standard, each specimen was subjected to an initial load (preload) of 10% of the test load for 1 hour at 570°C. The purpose of the preload is to ensure that the applied load is uniaxial along the specimen. After one hour, the 100% load can be applied. The temperature tolerance applied is ±2°C. Strain test data are measured using an LVDT (Linear Variable Differential Transformer) sensor mounted at the bottom of the machine.

Table 1. Chemical composition of Gr-91 (wt. %).

C	Mn	P	S	Si
0.30 - 0.60	≤ 0.020	≤ 0.010	0.20 - 0.50	0.20 - 0.50
Cr	**Mo**	**V**	**Nb**	**N**
8.00 - 9.50	0.85 - 1.05	0.18 - 0.25	0.06 - 0.10	0.030 - 0.070
Ni	**Al**	**Cu**	**B**	
≤ 0.40	≤ 0.020	≤ 0.25	≤ 0.001	

Figure 2. Welded plate of Gr-91.

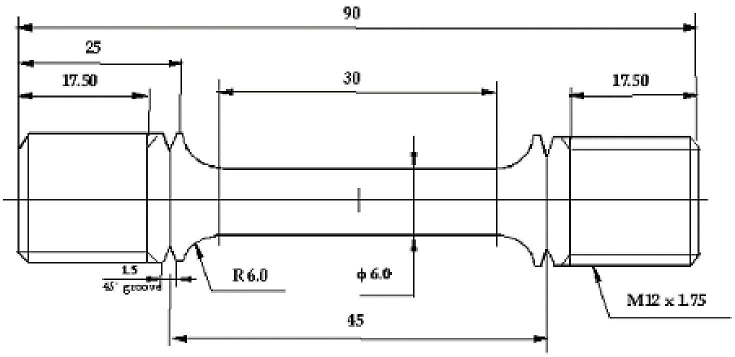

Figure 3. Dimension of creep specimen.

3. RESULT AND DISCUSSION

Figure 4 shows the creep curve characteristics for the BM, WJ, and HAZ specimens under a loading condition of 160 MPa at a temperature of 570°C. Under these conditions, all three specimen types exhibited curves with three typical creep deformation regions: primary (I), secondary (II), and tertiary (III). Typical creep deformation zones have been reported in previous studies for BM specimens [18]. For BM specimens, the total creep deformation time until fracture (primary through tertiary), tr, is 10,885 hours, while for WJ and HAZ specimens, it is 2,293 and 1,246 hours, respectively. All three specimen types exhibit similarities in the secondary zone, characterized by a higher percentage of creep deformation time than in the primary and tertiary zones. The phenomenon occurring in the secondary zone is the equilibrium between hardening and softening processes [18]. Significant differences in fracture time were observed in the creep test results between the BM specimen and the welded zones (WJ and HAZ). Degradation in the weld zone shortens the creep deformation until it eventually fractures suddenly. To quantitatively determine the impact of welding on creep resistance, a series of loading tests at 570 °C with varying loads was conducted, and the results were compared. By applying these loading variations, the deformation rate and creep mechanism can be determined.

Figures 5(a–c) show the creep strain rate versus time curves for the BM, WJ, and HAZ specimens, respectively, under a loading condition of 160 MPa. These curves were obtained by calculating the rate of change of creep deformation with respect to time (dℇ/dt). The creep strain rate can be determined in two ways: either from the minimum value in the secondary region or from the average of the primary, secondary, and tertiary regions. Calculating the strain rate based on the average value yields a more conservative result compared to the minimum value [9]. In this study, the creep strain rate was determined as the minimum value observed in each curve in Figure 5 (a–c). The minimum creep strain rate for each specimen was determined by drawing a horizontal line based on the density of the distribution of the lowest creep strain rate values. The minimum strain rate values for the BM, HAZ, and WJ specimens are 2.060E-7, 3.4019E-6, and 1.6323E-6 (1/h), respectively. To determine the trend of the creep strain rate under different loading conditions, the Norton equation was applied. The Norton equation is simply formulated as follows [7]:

$$\dot{\varepsilon}_{ss} = A(\sigma)^n \tag{1}$$

The values of A and n are the creep constant and exponent, respectively.

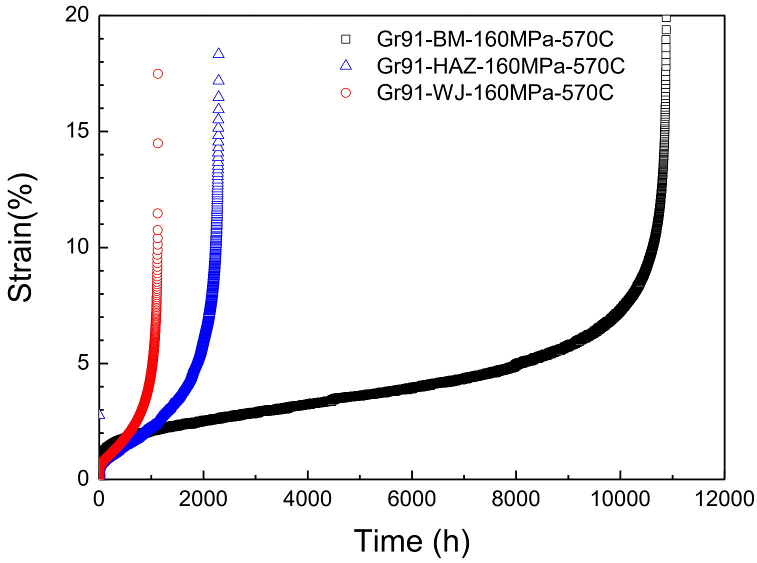

Figure 4. Typical creep curve at160 MPa; (a) BM, (b) HAZ, (c) WJ.

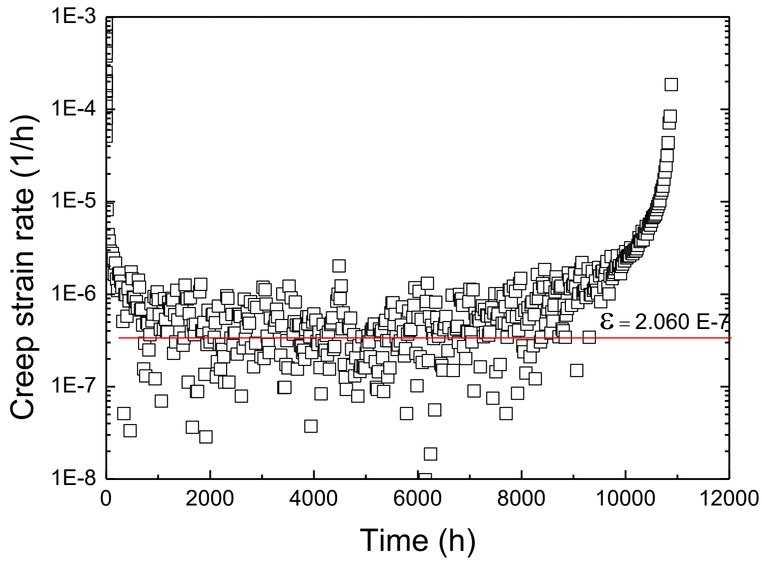

(a)

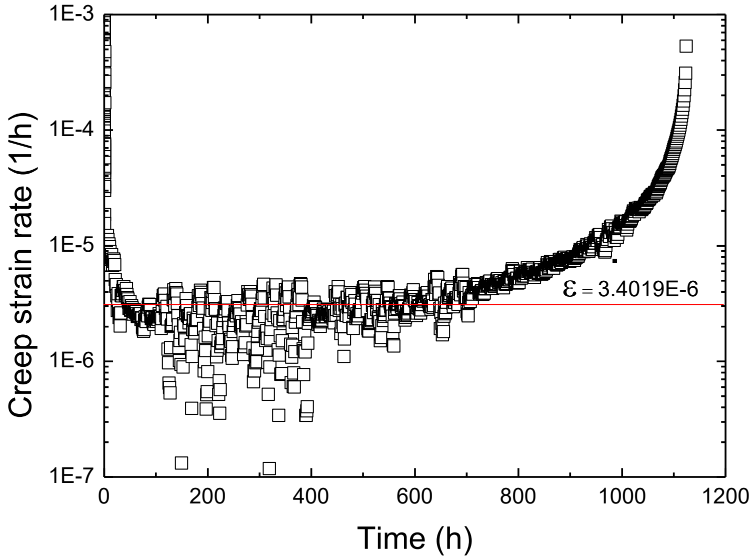

(b)

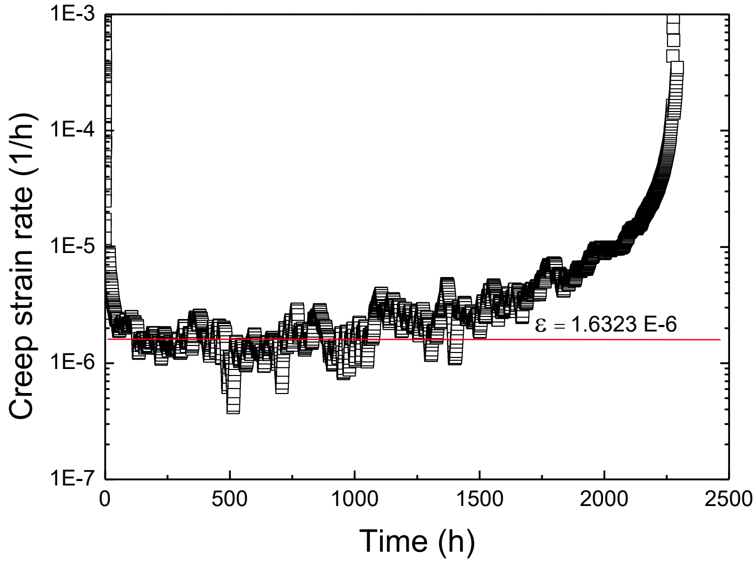

(c)

Figure 5. Minimum creep strain rate values during secondary creep at 160 MPa; (a) BM, (b) HAZ, (c) WJ.

The values of *A* and *n* represent the strain hardening coefficient and the creep exponent, respectively. Applying the Norton equation to each specimen yields the trend lines shown in Figures 6(a)–(c). The values of the constants *A* and *n* for the BM, HAZ, and WJ specimens are summarized in Table 2. It has been reported that the creep exponent, *n*, represents the mechanism of creep deformation [19][20]. In this study, the applied creep load range falls within the high-stress regime [20]. In the high-stress regime, creep exponent values reported in previous studies are greater than 11 [19], [20]. Meanwhile, in the low-stress regime, reported creep exponents range from 5 to 7 [19]. In the high-stress range, the creep deformation mechanism involved is dislocation climb. Dislocation climb occurs due to the presence of obstacles, such as precipitates $M_{23}C_6$, M_2N, and MX, during creep deformation. [21].

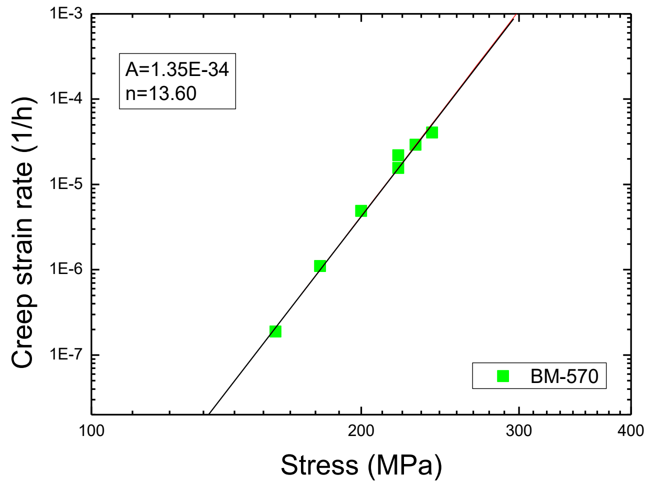

(a)

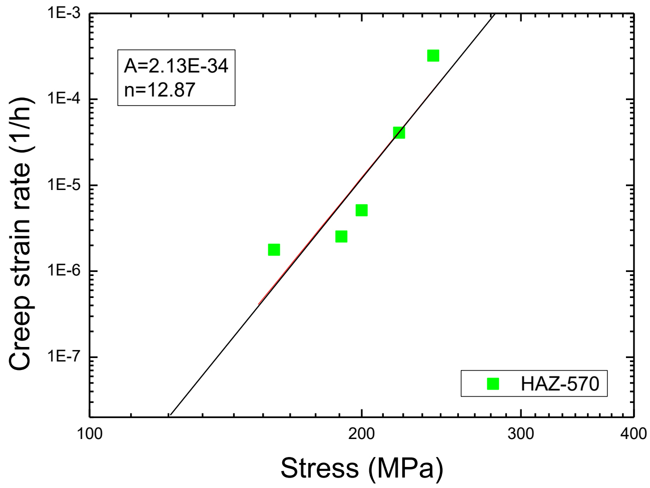

(b)

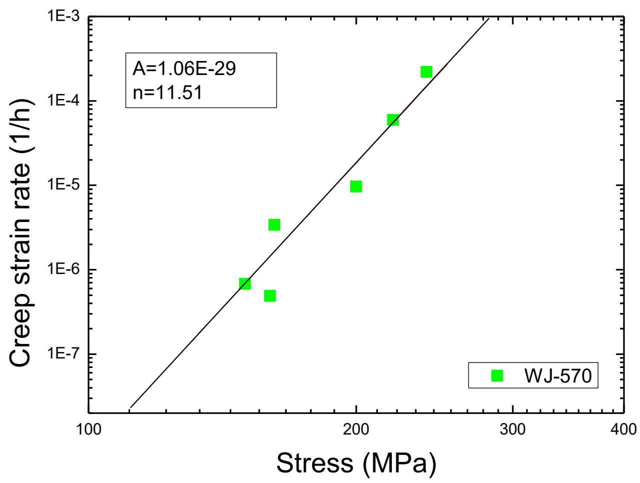

(c)

Figure 6. Creep strain rate to the applied load; (a) BM, (b) HAZ, (c) WJ.

Table 2. *S*train hardening coefficient *and* creep exponent for each specimen

	A	*n*
BM	1.35E-34	13.60
HAZ	2.13E-33	12.87
WJ	1.06E-29	11.51

Figure 7 compares predicted creep strain rates based on trendline extensions for the BM, HAZ, and WM specimens. High-load testing allows for the prediction of creep strain rates in the low-load range. In the BM specimen, the creep strain rate remained consistently lower than that of the HAZ and WJ specimens. An interesting finding is observed in the strain-rate trends of the HAZ and WJ. In the low-load category, the WJ strain rate showed a higher trend than that of the HAZ specimen. The HAZ strain rate intersects with WJ at approximately 180 MPa. Above a loading of 180 MPa, the HAZ strain rate showed a higher trend compared to WJ and was categorized as high loading. In the low-loading category, the creep heating duration was quite long. This extended duration caused the HAZ region to experience a strength increase due to excessive heating[14]. Conversely, the homogeneous regions, namely WJ and BM, underwent softening. This increases the potential for fracture in areas with a more homogeneous structure, namely WJ or BM. It has been reported that cracks occurring in homogeneous areas are classified as Type-I cracks [14]. Conversely, in the high-loading category, the short heating time leads to initial cracking in the HAZ. Cracks in the HAZ are classified as Type-IV cracks. The type of crack that occurs determines the strain rate in each area, as shown in Figure 7.

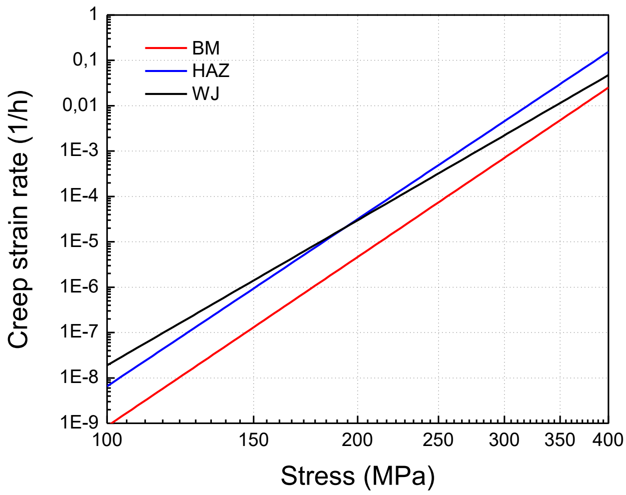

Figure 7. Comparison of creep strain rates under high and low loading conditions; (a) BM, (b) HAZ, (c) WJ.

4. CONCLUSIONS

In this study, the creep strain rate trends of Gr-91 steel in welded specimens were investigated. The creep strain rates at a temperature of 570 °C for the three welded areas, base metal (BM), heat-affected zone (HAZ), and weld joint (WJ), were obtained based on load variations under high-load conditions. Based on the strain rate values, the strain hardening coefficient and creep exponent can be determined by applying Norton's equation. The creep exponent values for all three specimen types were above 11, indicating a dislocation-climb mechanism for creep deformation. Furthermore, the highest creep strain rate was observed in the HAZ specimen under the high-load category, while under the low-load category, the highest creep strain rate was observed in the WJ specimen. The BM specimen consistently exhibited the lowest creep strain rate compared to the HAZ and WJ specimens in both the low- and high-load categories.

ACKNOWLEDGMENTS

This research was funded by LPPM Universitas Sanata Dharma through the 2025 competitive internal research grant scheme (No. 016 PeneI./LPPM-USD/IV2025).

REFERENCES

[1] D. Toma et al., “Preliminary Study on the Application for Monitoring Work Parameters in the Experimental Testing Facility under the Operating Conditions Generation IV Nuclear Reactors,” in 15th International Conference on Electronics, Computers and Artificial Intelligence, ECAI 2023 - Proceedings, Institute of Electrical and Electronics Engineers Inc., 2023. doi: 10.1109/ECAI58194.2023.10194103.

[2] “The Next Generation Nuclear Plant,” 2009.

[3] T. Denisa, N. A. Ionut, and B. Nicu, “Generation IV Nuclear Energy Systems-Alternative Solutions to Carbon Emission Energy Sources,” in 2022 14th International Conference on Electronics, Computers and Artificial Intelligence, ECAI 2022, Institute of Electrical and Electronics Engineers Inc., 2022. doi: 10.1109/ECAI54874.2022.9847457.

[4] N. Chaudhari, “Nuclear Power Reactor- An Overview,” Saudi Journal of Engineering and Technology, vol. 8, no. 07, pp. 155–162, Jul. 2023, doi: 10.36348/sjet.2023.v08i07.001.

[5] T. J. Katona, Á. Biro, and S. Rátkai, “Feasibility of Safe Operation of WWER-440-Type Nuclear Power Plants for Up to 60–70 Years,” May 01, 2023, MDPI. doi: 10.3390/en16104170.

[6] I. L. Pioro and G. H. Rodriguez, “Generation IV International Forum (GIF),” Handbook of Generation IV Nuclear Reactors: A Guidebook, pp. 111–132, Jan. 2023, doi: 10.1016/B978-0-12-820588-4.00010-4.

[7] Y. Yamaguchi, J. Katsuyama, Y. Kaji, M. Osaka, and Y. Li, “Expansion of High Temperature Creep Test Data for Failure Evaluation of BWR Lower Head in A Severe Accident,” in International Conference on Nuclear Engineering, Proceedings, ICONE, American Society of Mechanical Engineers (ASME), May 2019. doi: 10.1299/mej.19-00560.

[8] M. Jakubowska, R. Chulist, L. Maj, and A. Sypien, “Analysis of the Creep Mechanism of Low-Alloy Steel in Terms of Plastic Deformation,” J Mater Eng Perform, Dec. 2024, doi: 10.1007/s11665-024-10229-8.

[9] I. M. W. Ekaputra, “Prediksi Laju Perambatan Retak Melar Pada Baja Austenitik 316L Menggunakan Data Uji Melar Dan Metode NSW,” 2019.

[10] J. H. Fu et al., “Creep Reliability Assessment of Structural Components at Elevated Temperatures Considering The Time Dependent Feature of Representative Stress,” Eng Fract Mech, vol. 310, Nov. 2024, doi: 10.1016/j.engfracmech.2024.110458.

[11] I. M. W. Ekaputra, W. G. Kim, J. Y. Park, S. J. Kim, and Y. W. Kim, “Analysis of The Creep Crack Growth Rate for Modified 9Cr-1Mo Steel Using Q* Parameter,” Journal of Mechanical Science and Technology, vol. 28, no. 10, pp. 4075–4081, Oct. 2014, doi: 10.1007/s12206-014-0920-x.

[12] M. Purnama and U. Sudjadi, “Mechanical Study of 9Cr-316SS-1Mo Materials For Nuclear Fuel Cladding Materials Power Reactors,” International Journal of Innovation in Mechanical Engineering and Advanced Materials, vol. 4, no. 2, p. 38, Feb. 2023, doi: 10.22441/ijimeam.v4i2.16832.

[13] W. Zhang et al., "An Engineering Approach for Weld Creep Lifetime Assessment Based on Local Property Measurement," 2024, doi: 10.31399/asm.cp.epri2024p1320.

[14] Y. Wang, L. Li, and R. Kannan, "Transition from Type IV to Type I Cracking in Heat-Treated Grade 91 Steel Weldments," Materials Science and Engineering: A, vol. 714, pp. 1–13, Jan. 2018, doi: 10.1016/j.msea.2017.12.088.

[15] E. Isaac Samuel, B. K. Choudhary, and W. G. Kim, "Reliability Analysis on Long-Term Creep Life Prediction of Grade 91 Steel Weld Joints," 2016. Accessed: Jan. 09, 2025. [Online]. Available: https://inis.iaea.org/search/search.aspx?orig_q=RN:47104179

[16] F. Abe, "Grade 91 Heat-Resistant Martensitic Steel," Coal Power Plant Materials and Life Assessment: Developments and Applications, pp. 3–51, Jul. 2014, doi: 10.1533/9780857097323.1.3.

[17] "Test Methods for Conducting Creep, Creep-Rupture, and Stress-Rupture Tests of Metallic Materials," Jun. 01, 2018, ASTM International, West Conshohocken, PA. doi: 10.1520/E0139-18.

[18] I. M. W. Ekaputra, "Investigasi Laju Regangan Creep Baja Tahan Karat Ferritic Pada Temperatur 570 °C," Jurnal Rekayasa Mesin, vol. 15, no. 3, pp. 1655–1663, Dec. 2024, doi: 10.21776/jrm.v15i3.1848.

[19] K. Guguloth and N. Roy, "Creep Deformation Behavior of 9Cr1MoVNb (ASME Grade 91) Steel," Materials Science and Engineering: A, vol. 680, pp. 388–404, Jan. 2017, doi: 10.1016/j.msea.2016.10.112.

[20] B. K. Choudhary, "Tertiary Creep Behaviour of 9Cr-1Mo Ferritic Steel," Materials Science and Engineering: A, vol. 585, pp. 1–9, Nov. 2013, doi: 10.1016/j.msea.2013.07.026.

[21] K. H. Lee, J. Y. Suh, S. M. Hong, J. Y. Huh, and W. S. Jung, "Microstructural Evolution and Creep-Rupture Life Estimation of High-Cr Martensitic Heat-Resistant Steels," Mater Charact, vol. 106, pp. 266–272, Jun. 2015, doi: 10.1016/j.matchar.2015.06.005.